Influence of the supporting surface inclination angle of the external geokhod propulsor on the deflected mode of boundary rock massif

V Yu Beglyakov[1,2], V V Aksenov[1,2], I K Kostinets[3], A B Efremenkov[4] and A A Khoreshok[5]

[1] National Research Tomsk Polytechnic University, Yurga Institute of Technology, Yurga, 652050, Kemerovo Area, Yurga, ulitsa Leningradskaya, 26
[2] Institute of Coal of the Siberian Branch of the Russian Academy of Science 650000, Kemerovo, prospect Sovetski, 18
[3] Branch of Kuzbass State Technical University named after T.F. Gorbachev in Belovo town, 652644, Kemerovo Area, Belovo, urban-type community Inskoy, ulitsa Ilyicha, 32a
[4] Novgorod State University, ul. B. St. Petersburgskaya, 41 173003 Veliky Novgorod, Russia
[5] T.F. Gorbachev Kuzbass State Technical University, 650000, Kemerovo, ulitsa Vesennyaya, 28

E-mail: abe@novsu.ru
E-mail: begljakov@rambler.ru

Abstract. The article describes the interaction model of the external propulsor propeller blade of the geokhod with boundary rock massif. The model makes it possible to investigate the influence of the supporting surface inclination angle of the external geokhod propulsor on the deflected mode of boundary rock massif. The results of modeling and their analysis are given. The ways of optimization of supporting surface geometrical parameters are outlined.

One of the key processes that occur in the underground geodetic mining is the geokhod screwing into rock massif [1-4]. In this case the direction of the interaction force between the propeller blade and the rock is determined by the location of the blade supporting surface (Figure 1), namely, the angle of its inclination in relation to the frontal plane.

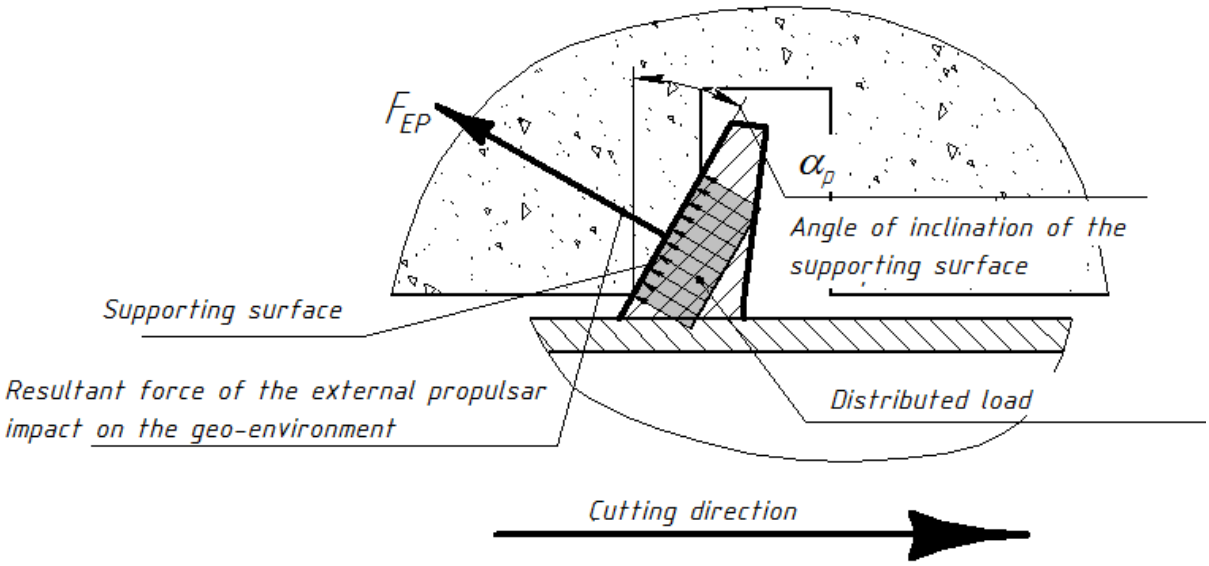

Figure 1. Interaction scheme of the external propulsor propeller blade of the geokhod with geo-environment.

The inclination angle also depends on the value of the interaction force [5, 6]. With $\alpha_p = 0$ the force of interaction is at its minimum, but there is a higher probability of cleavage or shearing of the inter-turn block. As the angle increases, the stresses are shifted towards the compression [7-9], but the forces of interaction increase [5, 6]. That is, the angle $\alpha_p$has an ambiguous effect on the bearing capacity of the boundary rock massif [6].

Therefore, the problem that arises is to investigate the effect of the supporting surface inclination angle α_p of the external propulsor (EP) on the deflected mode of the boundary rock massif.

To assess the influence of the inclination angle $\alpha_p$of the supporting surface, a model of the working area with a two-path system of circumscribed helical channels was created. The scheme of the model is shown in Figure 1.

In modeling, the upper limit of the values of the inclination angle α_p of the supporting surface was assigned to 54°, which corresponded to the theoretical angle of the seizure of the geokhod in the output [6]. The angle α_p varied in the range from 0 to 50° in steps of 5° and in the range from 50 to 54° in steps of 1°.

To exclude their influence, the following parameters remained unchanged: the depth of the boundary channels H = 0.25 m, the pitch of the helical line of the external propulsor $h_в$ = 0.8 m, the length of the supporting surface along the output contour l = 1 m and the position of the free surface.

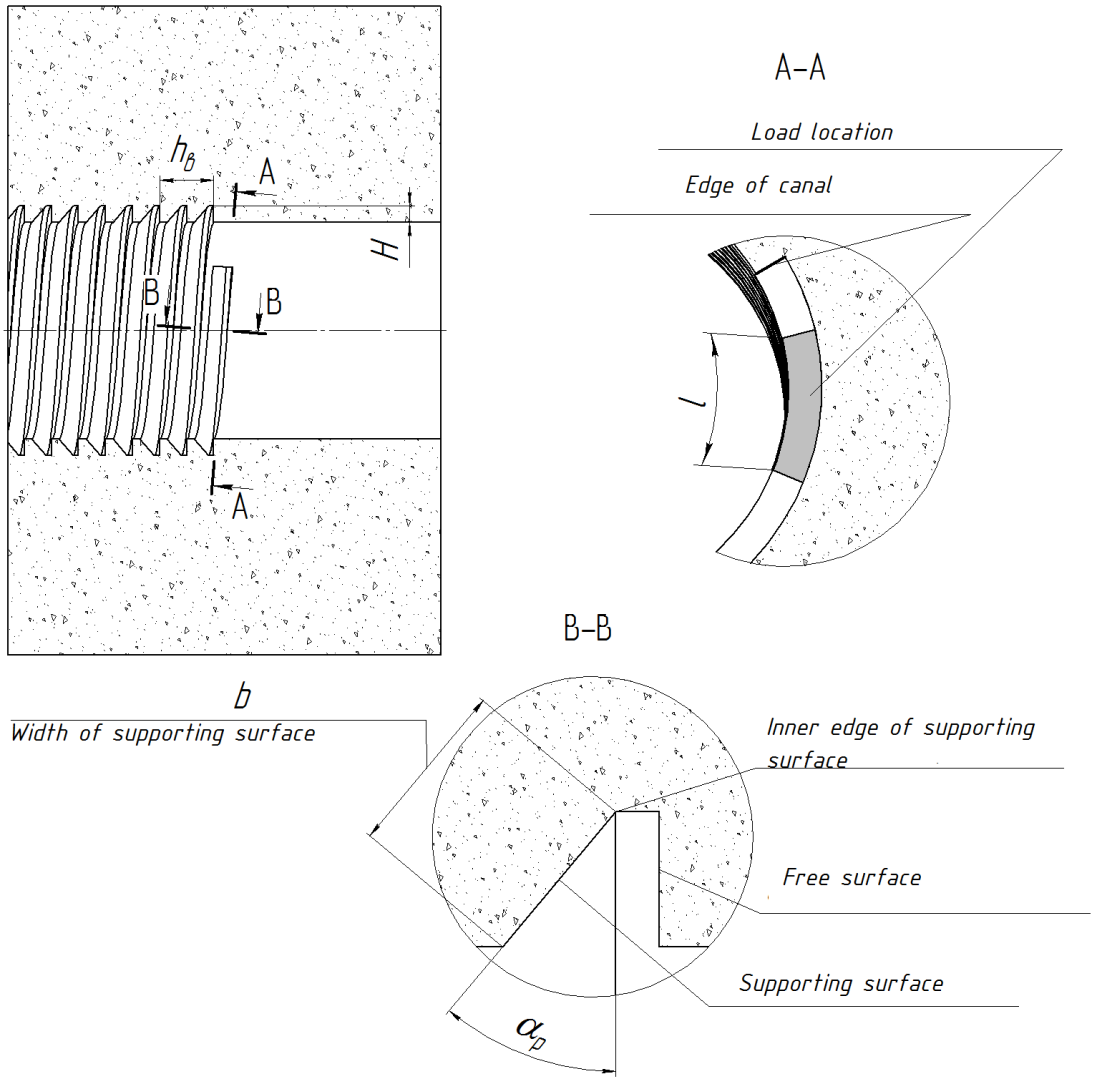

Figure 2. General view of the model for assessing the influence of the supporting surface inclination angle of the external propulsor on the deflected mode of the boundary rock massif.

The model simulated the operating conditions of the two-way external propulsor [10-12], the load was applied to the supporting surfaces of the channels, the leading edge of the supporting surface was located 500 mm from the bottom of the boundary channel.

The models were divided into three 10-node finite elements [13, 15]. The contact surfaces of the boundary rock massif with the external propulsor blades and the adjacent areas were divided into 50 mm elements, the rest of the model was divided into 500 mm elements, the transition of the element sizes from 50 to 500 mm was carried out on four transition layers [16] (Figure 3).

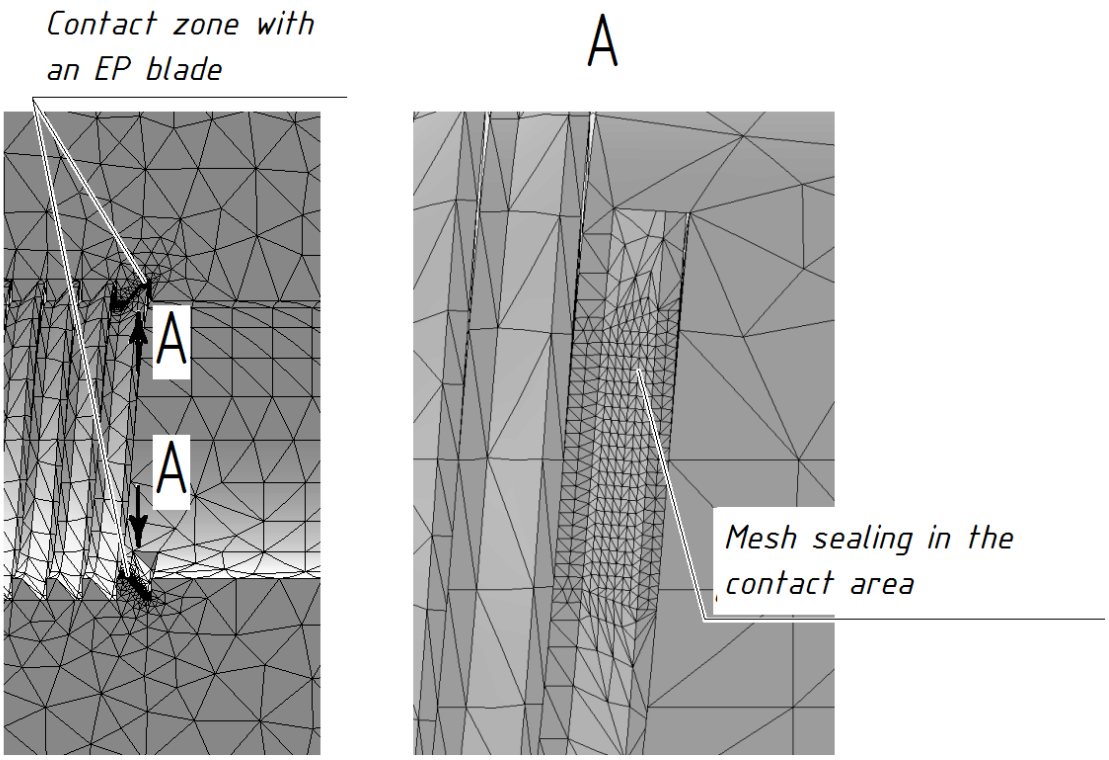

Figure 3. The grid of partitioning the model into finite elements.

A normal and tangential load was applied to the contact surface of the blade with the boundary rock massif (Figure 4) with intensities

$$q_n = \frac{F_{EP}^N}{S_{SS}} \text{ and } q_t = \frac{F_{EP}^{FF}}{S_{SS}}$$

Where F_{EP}^N is the normal force acting on the side of the blade, F_{EP}^{FF} is the blade's friction force on the rock, S_{SS} the contact area of the blade with the rock. The values of the forces F_{EP}^N and F_{EP}^{FF} depended on the inclination angle of the supporting surface and were determined from the mathematical model given in [6], the values of the areas S_{SS} at different angles α_p were measured on the model.

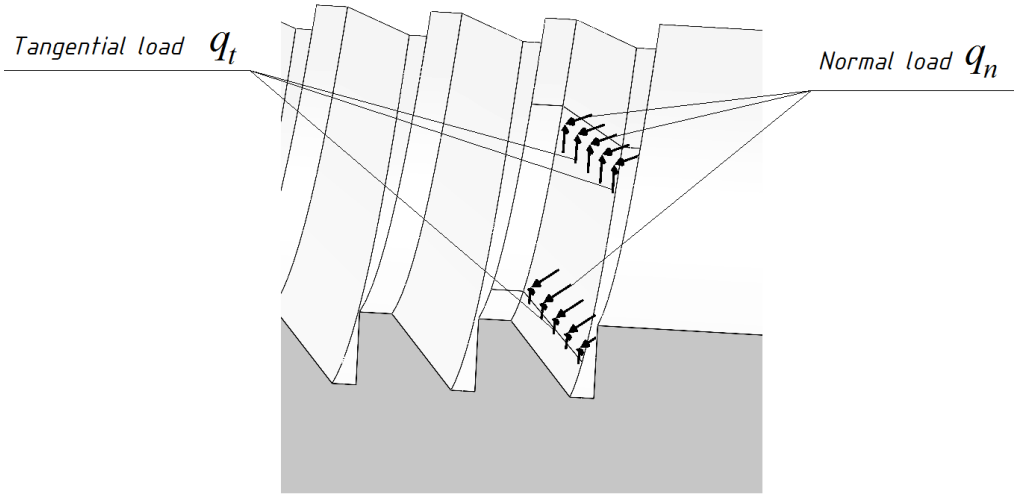

Figure 4. The scheme of applying the load to the model

In the course of preliminary modeling, different types of deflected mode in the area of interaction with the blade were evaluated. Three diametrical cross-sections were considered when assessing the rock deflected mode: at the anterior edge of the blade (III-III), in the middle of the blade (II-I) and at the posterior edge of the blade (I-I) (Figure 5).

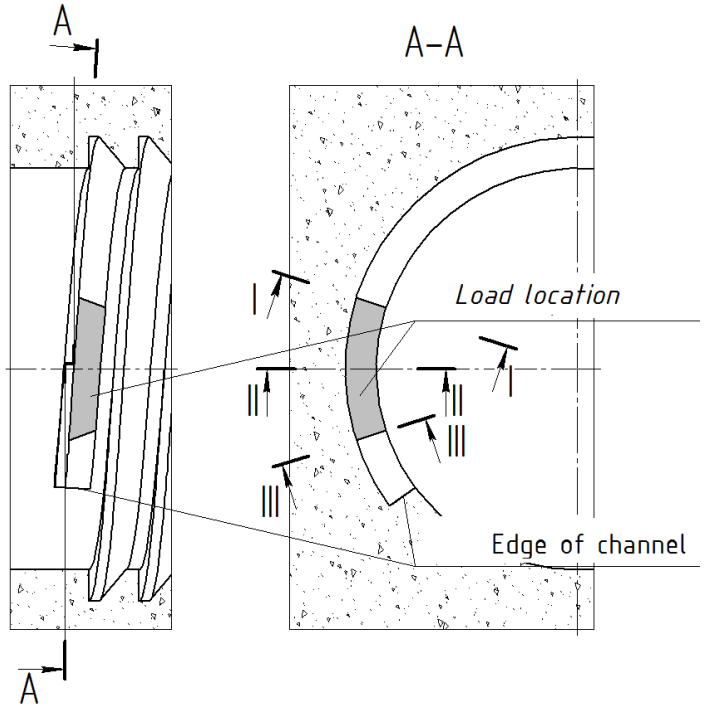

Section I-I - at the posterior edge of the blade, II-II - in the middle of the blade,
III-III - at the anterior edge of the blade

Figure 5. Diagram of diametrical cross sections arrangement on the model

The assessment of the deflected mode was carried out visually according to the diagrams of the main stresses σ_1, σ_1 and tangential stresses τ at angles of inclination of the reference surface from 0° to 40° in steps of 10°. Stress diagrams in section II-II for some angles α_p are shown in Figure 6.

From stress diagrams in diametrical cross sections, it can be seen that the maximum stresses occur on the contact surface and decrease with removal in depth. At values of the angle $\alpha_p > 20°$ the stress moduli increase with increasing angle.

Also, during preliminary modeling, the stress distribution along the reference surface was visually assessed.

Figure 7 shows the diagrams of the distribution of principal and tangential stresses over the contact surface.

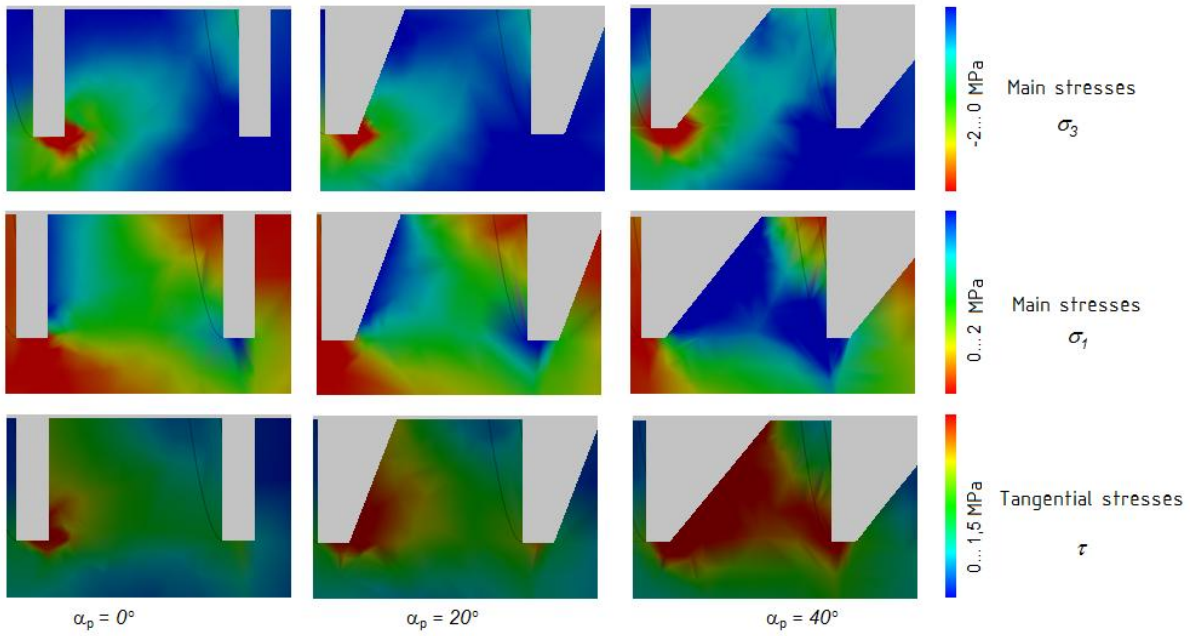

Figure 6. Stress diagrams in the middle section of the reference channel surface

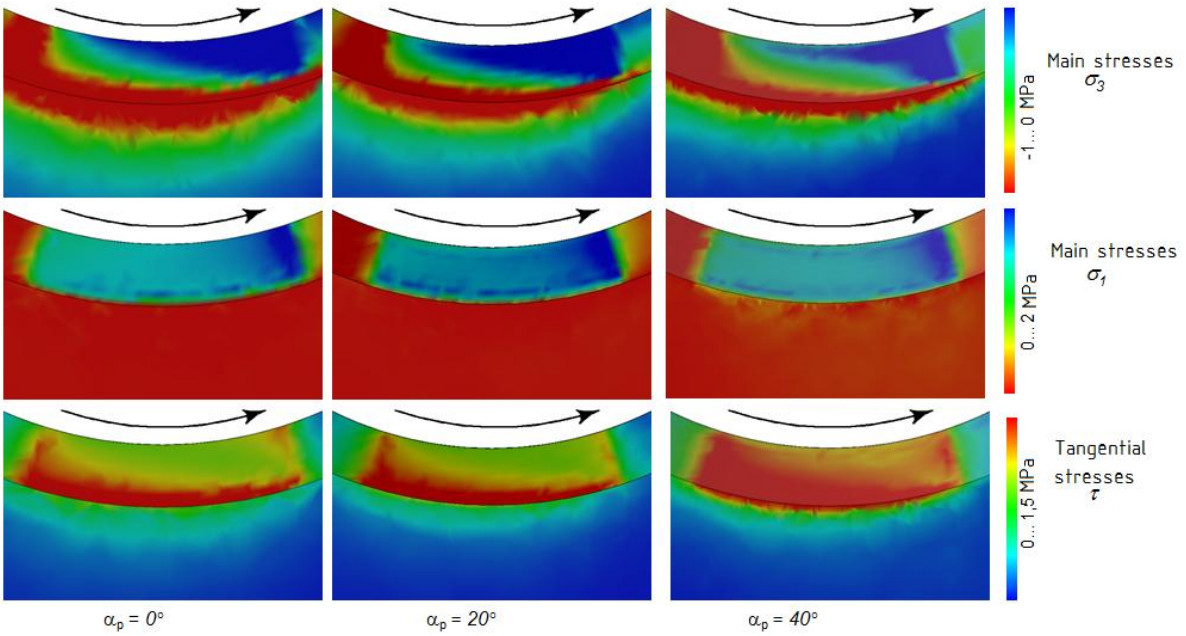

Figure 7. Distribution of stresses along the supporting surface of the boundary channel

From the stress distribution diagrams along the supporting surface of the channel it is seen that the compressive stress prevails in the area of the anterior edge of the blade, and the blades in the area of the posterior edge of the blade are stretching. Tangential stresses grow from the anterior to posterior margin of the blade. The change in stress from the anterior to posterior edges of the blade is monotonous. At values of the angle $\alpha_p > 20°$ the stress modules increase with increasing angle.

With further modeling, the influence of the angle $\alpha_p$on the stresses in the rock at various points of the reference surface was investigated.

Figure 8 shows the layout of the control points on the reference surface.

During the simulation, the main stresses σ_1 and σ_3, tangential stresses τ and equivalent stresses σ_{equV} were determined on the interaction surface of the blade with the boundary rock massif, and the stress distributions over the surface were compared for different angles of inclination α_p.

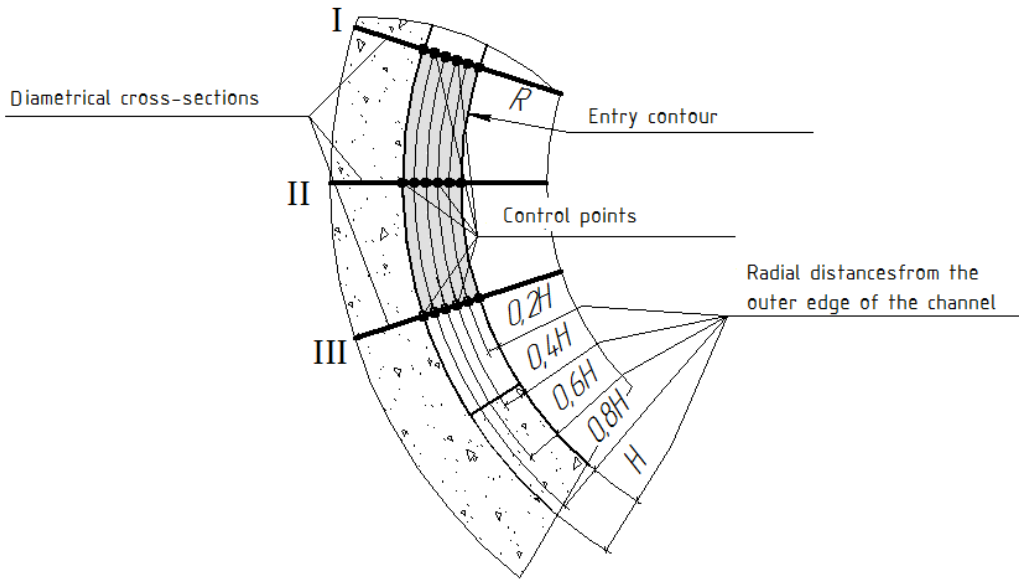

Figure 8. Scheme for placing control points on the supporting surface of the boundary screw channel.

Equivalent stresses were determined by the theory of Mohr strength according to the formulas [17]:
- for areas with positive stresses σ_1 and negative ones σ_3:

$$\sigma_{equV} = \sigma_1 - \frac{[\sigma]_C}{[\sigma]_P}\sigma_3$$

- for triaxial compression areas: $\sigma_{equV} = \sigma_1 - \sigma_3$

- for triaxial stretching areas: $\sigma_{equV} = -\frac{[\sigma]_C}{[\sigma]_P}\sigma_3$

where $[\sigma]_C$ and $[\sigma]_P$ are the ultimate strength of the rock massif to uniaxial compression and stretching, respectively.

Numerical results of the simulation are presented in the form of graphical dependencies in Figures 9 ... 12, which reflect the influence of the angle α_P of the supporting surface inclination of the external propulsor propeller blade on the distribution of stresses along the supporting surface of the screwed channel.

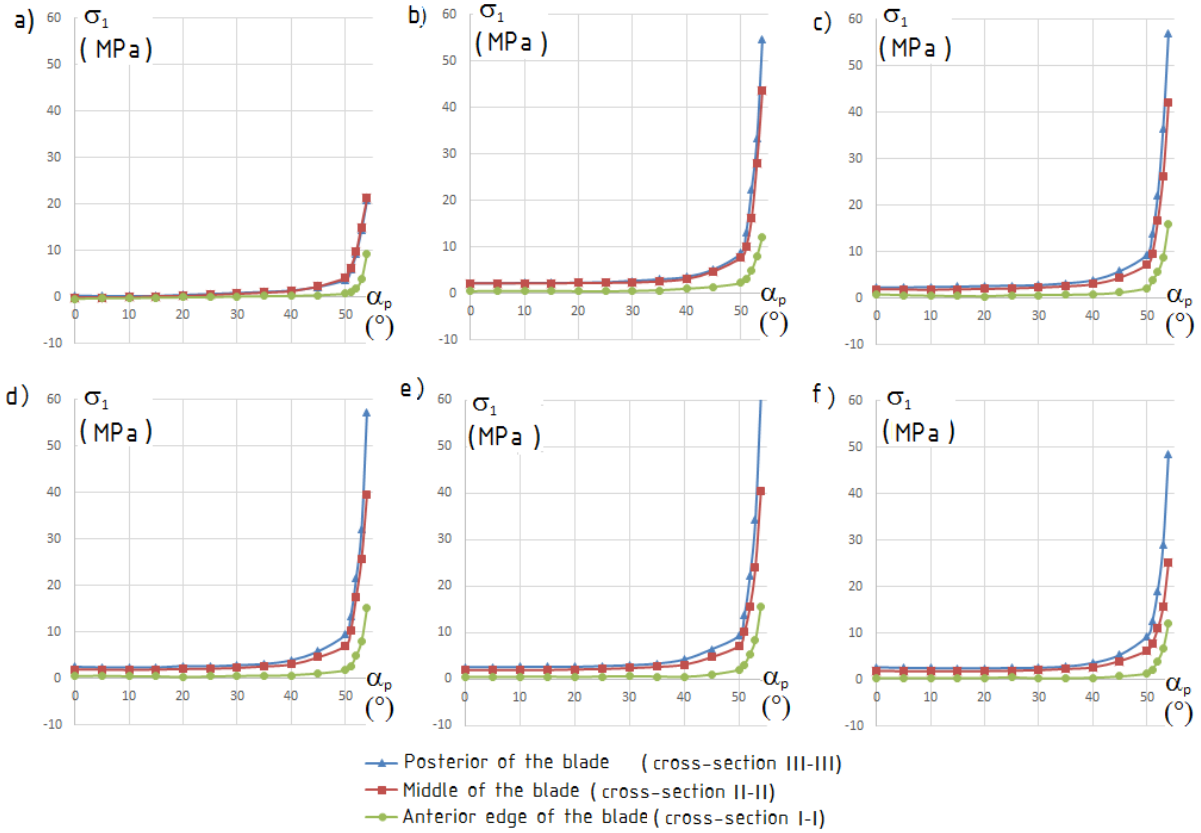

a) at the inner edge, b) at a distance of 0.8 H from the outer edge, c) at a distance of 0.6 H from the outer edge, d) at a distance of 0.4 H from the outer edge, e) at a distance of 0.2 H from the outer edge, f) in the area of the outer edge

Figure 9. Dependence of the main stresses σ_1 on the inclination angle of the supporting surface α_P .

The family of curves in Figure 9 reflects the dependence of the principal stresses σ_1 on the inclination angle α_P of the supporting surface of the external propulsor propeller blade. It can be seen from the graphs in Figure 6 that with increasing angle α_P in the range from 0 to 25 degrees, the values of the principal stresses σ_1 decrease slightly, with further increase in the angle α_P, the stress values σ_1 increase. In the range of angles α_P from 0 to 30 degrees, the main stresses σ_1 are slightly dependent on the angle α_P, at angles α_P greater than 50 degrees there is a sharp increase in stress. In the area of the inner edge at angles α_P less than 20 degrees there are negative stress values σ_1, which indicates the presence of areas with triaxial stretching in this area.

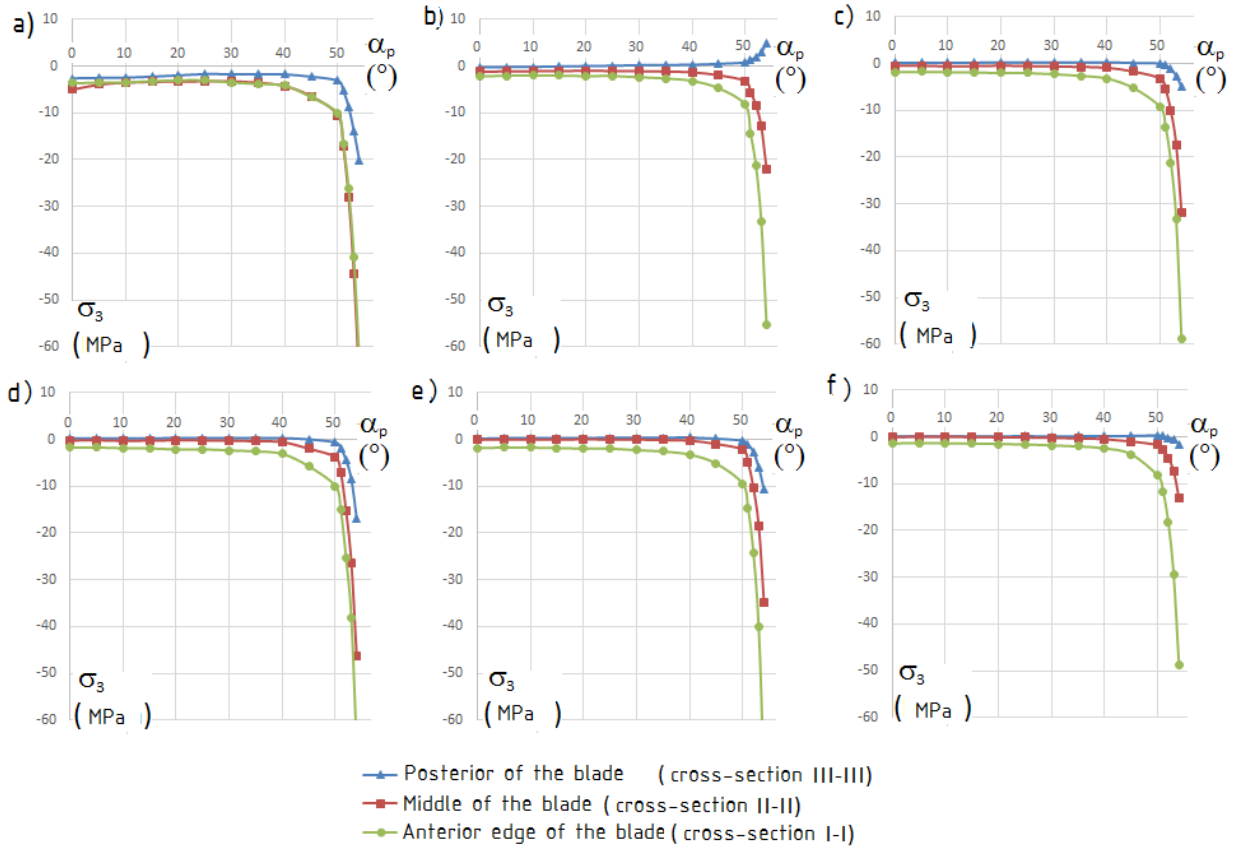

a) at the inner edge, b) at a distance of 0.8H from the outer edge, c) at a distance of 0.6H from the outer edge, d) at a distance of 0.4H from the outer edge, e) at a distance of 0.2 H from the outer edge, f) in the area of the outer edge

Figure 10. Dependence of the main stresses σ_3 on the inclination angle of the supporting surface α_P

The family of curves in Figure 10 reflects the dependence of the main stresses σ_3 on the inclination angle α_P of the supporting surface of the external propulsor blades. From the graphs in Figure 7, we conclude that with increasing angle α_P in the range from 0 to 25 degrees, the values of the principal stresses σ_3 shift slightly in the direction of compression, with further increase in the angle α_P, the stress values σ_3 shift towards stretching. In the range of angles α_P from 0 to 30 degrees, the main stresses σ_3 are weakly dependent on the angle α_P, at angles α_P greater than 50 degrees there is a sharp increase in the stress modules, the stresses are shifted towards the stretching. In the area of the leading edge of the external propulsor blades, positive stress values σ_3 occur, indicating that there are areas with triaxial compression in this area.

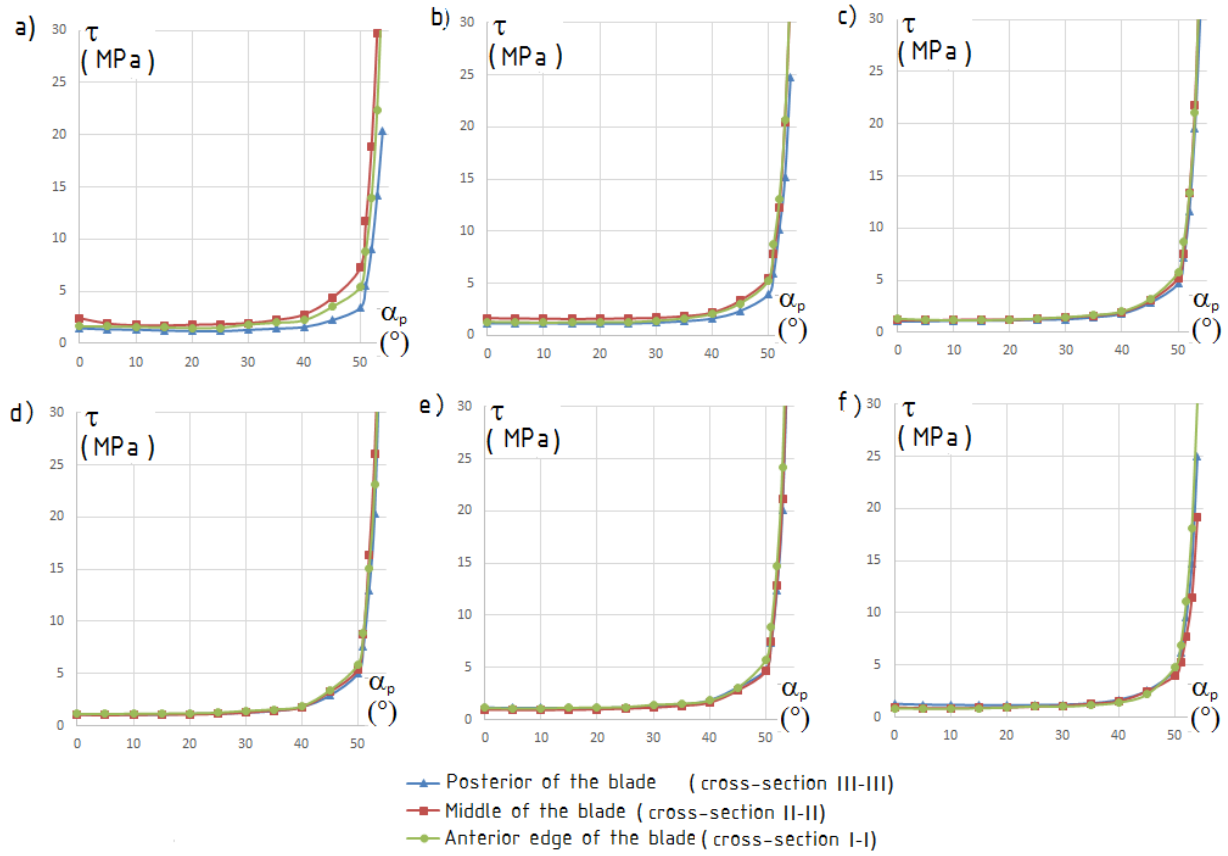

a) at the inner edge, b) at a distance of 0.8 H from the outer edge, c) at a distance of 0.6 H from the outer edge, d) at a distance of 0.4 H from the outer edge, e) at a distance of 0.2 H from the outer edge, f) in the area of the outer edge

Figure 11. Dependence of tangential stresses τ on the inclination angle of the supporting surface α_P

The family of curves in Figure 11 reflects the dependence of tangential stresses on the inclination angle of the supporting surface of the external propulsor blade. From the graphs in Figure 8, we conclude that with increasing angle in the range from 0 to 15 degrees, the tangential stress values decrease slightly, with further increase in the angle, the stress values increase. In the range of angles from 0 to 30 degrees, the tangential stresses are slightly dependent on the angle, at angles greater than 50 degrees there is a sharp increase in stresses. When moving from the leading edge of the blade to the rear, there is an insignificant increase in tangential stresses.

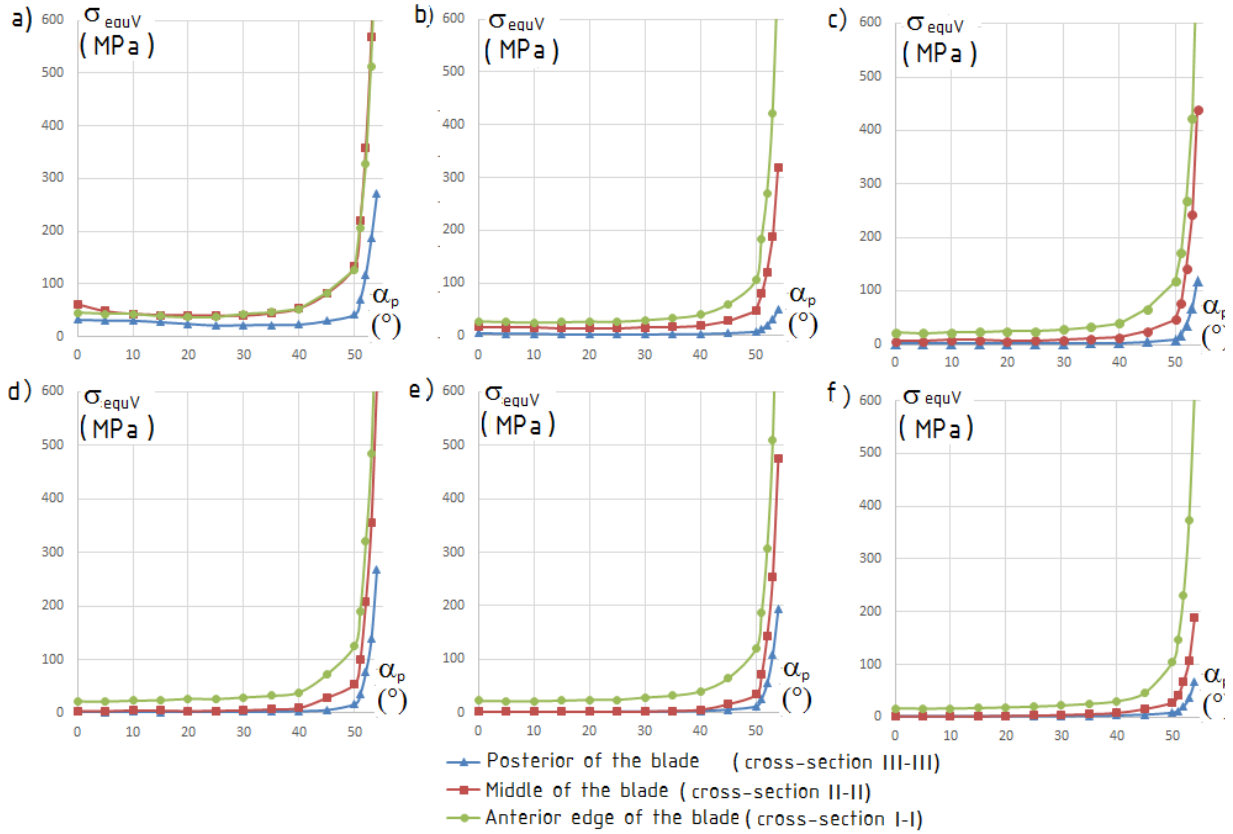

a) at the inner edge, b) at a distance of 0.8 H from the outer edge, c) at a distance of 0.6 H from the outer edge, d) at a distance of 0.4 H from the outer edge, e) at a distance of 0.2 H from the outer edge, f) in the area of the outer edge

Figure 12. Dependence of equivalent stresses σ_{equV} on the inclination angle of the supporting surface α_P .

The family of curves in Figure 12 reflects the dependence of the equivalent stresses on the inclination angle of the supporting surface of the external propulsor blades. From the graphs in Figure 12 we conclude that with increasing angle in the range from 0 to 20 degrees, the values of equivalent stresses decrease slightly, with further increase in the angle, the stress values increase. In the range of angles from 0 to 30 degrees, equivalent stresses are weakly dependent on the angle, at angles greater than 50 degrees there is a sharp increase in stresses. When moving from the leading edge of the blade to the rear, equivalent stresses grow.

The following conclusions can be drawn from the studies:

- when designing external geostatic propulsors it is advisable to take measures to shift the maximum loads to the front edge of the blade and partially unload the rear edge of the blade.
- the dependence of stresses on the inclination angle of the supporting surface is nonmonotonic in nature, i.e. there is an angle at which the crushing probability of the reference surface of the channel is minimal, this angle depends on the point position on the support surface;
- the use of inclination angles of more than 30 degrees is inappropriate, since it leads to an unconditional increase in stresses in the rock and interaction forces;
- with further research it is advisable to consider the range of angles from 0 to 30 degrees.

References

[1] Aksenov V V, Khoreshok A A , Efremenkov A B , Kazantsev A A , Beglyakov V Yu and Walter A V 2015 Sozdanie novogo instrumentariya dlya formirovaniya podzemnogo prostranstva [Creation of a new instrument for the underground space formation] *Gornaja tekhnika [Mining machinery (Catalog-reference book)]* (St. Petersburg) **1**(15) 24-26
[2] Begljakov V Yu and Aksenov V V 2012 *Poverhnost' zaboja pri prohodke gornoj vyrabotki geohodom [A surface of the face during the mining of the mine by the geokhod]* (Saarbrucken: LAP LAMBERT Academic Publishing GmbH & Co. KG) 139
[3] Aksenov V V, Sadovets V Yu and Beglyakov V Yu 2009 Influence of the dynamic processes formed in operating conditions on the power parameters of the knife executive body *Mining information-analytical bulletin* (scientific and technical journal). Vol. 10, **12**, 91-106.
[4] Aksenov V V, Beglyakov V Yu, Kazantsev A A, Walter A V and Efremenkov A B 2016 Opyt uchastija v proekte po organizatsii vysokotehnologichnogo proizvodstva [Experience in the project on the organization of high-tech production] *Mining equipment and electromechanics*. **8** (126) 8-15
[5] Beglyakov V Yu, Aksenov V V, Kostinets I K and Khoreshok A A 2017 Shemy nagruzhenija pri modelirovanii protsessa vzaimodejstvija vneshnego dvizhitelja geohoda prikonturnym massivom porod [Loading schemes for modeling the process of interaction of an external propeller of the geodatabase by an boundary rock massif of rocks] *Mining sciences and technologies* **3** 3-10
[6] Beglyakov V Yu, Aksenov V V, Kostinets I K and Khoreshok A A 2017 Determination of the interaction forces of the main systems of the geokhod with the geoenvironment and with each other *Mining sciences and technologies* **4** 23-30
[7] Aksenov V V, Kostinets I K, Beglyakov V Yu 2012 Influence of the inclination angle of the interaction surface between the executive part of the geokhod and the rock of the face on its stress-strain state *Mining information analytical bulletin* (scientific and technical journal) **2** 30-36.
[8] Aksenov V, Sadovets V Yu, Buyalich G D and Beglyakov V Yu 2011 Influence of the ledge on the deflected mode of the bottomhole part of the mine workings *Mountain Information and Analytical Bulletin* (scientific and technical journal) Ed. **2**: Mining machinery 55-67
[9] Aksenov V V, Efremenkov A B and Beglakov V Yu 2011 Modeling of the stressed-deformed state of the rock created by the action of the executive body of the mining machine on it *Mining information-analytical bulletin* (scientific and technical journal) S**5** 9-14.
[10] Aksenov V V, Beglyakov V Yu, Kazantsev A A, Kostinets I K and Koperchuk A V 2016 Classification of geometric parameters of an external propeller of a geokhod *Mining equipment and electromechanics* **8** (126) 33-39
[11] Aksenov V V, Kostinets I K, Beglyakov V Yu 2012 Substantiation of the need to create an external propulsion device for emergency rescue workings *Mining Information and Analytical Bulletin* (scientific and technical journal) S**6** 110-114.
[12] Aksenov V V, Kostinets I K, Beglyakov V Yu 2013 Work Features of the geokhod external propeller *Mining information-analytical bulletin* (scientific and technical journal) S**6** 419-425
[13] Gallagher R 1984 *Metod konechnyh `elementov. Osnovy* [*The finite element method. Fundamentals]* (Moscow, Publ Mir [The World]) 428
[14] Alyamovskiy A A 2004 *SolidWorks. Engineering analysis by the finite element method* - Moscow: DMK Press] 432
[15] Fadeev A B 1987 *Metod konechnyh `elementov v geomehanike* [*Finite Element Method in Geomechanics]* (Moscow, Publ Nedra) 221
[16] Beglyakov V Yu, Aksenov V V, Kazantsev A A, Kostinets I K 2017 Development of a perimeter support-propulsion system of geokhods *Bulletin of the Kuzbass State Technical University* **6** (124)
[17] Aleksandrov A V, Potapov V D and Derzhavin B P 2009 *Soprotivlenie materialov* [Strength

of materials] *(*Moscow: Higher School) 560